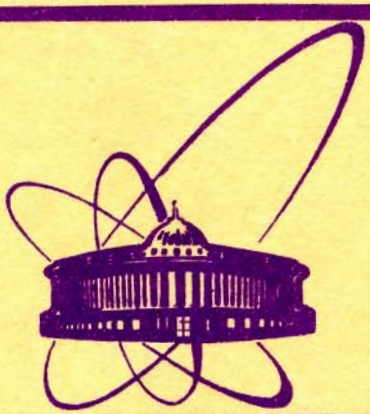

сообщения
объединенного
института
ядерных
исследований
дубна

E2 - 12844

S.Drenska, S.Cht.Mavrodiev

ON MODELLING OF HADRON INTERACTIONS

1979

E2 · 12844

S.Drenska, S.Cht.Mavrodiev

ON MODELLING OF HADRON INTERACTIONS

Дренска С., Мавродиев С.Щ.

E2 - 12844

О моделировании адронных взаимодействий

На основе понятия об эффективном радиусе взаимодействия дано описание полных сечений адрон-адронных взаимодействий. Исследована зависимость полных сечений от квантовых чисел сталкивающихся адронов. Предсказано поведение полных сечений, в том числе и адрон-ядерных взаимодействий, при энергиях, недоступных на современных ускорителях.

Работа выполнена в Лаборатории теоретической физики ОИЯИ

Сообщение Объединенного института ядерных исследований. Дубна 1979

Drenska S., Mavrodiev S.Cht.

E2 - 12844

On Modelling of Hadron Interactions

On the basis of the idea about the effective radius a description of the total cross sections of the hadron interactions is given. The dependence of the total cross sections on the quantum numbers of the colliding systems is investigated. The behaviour of the total cross sections, including the hadron-nuclear interactions is predicted at the energies that are impossible for the modern accelerators.

The investigation has been performed at the Laboratory of Theoretical Physics, JINR.

Communication of the Joint Institute for Nuclear Research. Dubna 1979

The problem of understanding the elementary particle dynamics puts forward alongside with the development of the general ideas of quantum field theory also the preliminary problem of the systematization of the elementary particles[1] and the experimental data of their interaction.

In this paper a possibility is considered for a simple and physical clear modelling of hadron interaction. It is based on the geometrical generalization of the Rutherford formula:

$$T(\vec{q}) = -\frac{m}{4\pi} \int d^3r \; T(\vec{r})\, e^{-i\,qr} \quad ,$$

where $\vec{r}$ is the relative coordinate, $\vec{q}$ is the relative momentum, and $T(\vec{q})$, $T(\vec{r})$ are the elastic scattering amplitude in momentum and coordinate representation. The connection between three-dimensional relative momentum and coordinate spaces has a simple group-theoretical sense. It is a reduction of the regular representation of the group of motion of momentum space into irreducible representations defined in the coordinate space. Consequently, if the geometry of the relative momentum space for some two-particle problem is known the above group theoretical construction can be used to define the relative coordinate space.

In agreement with the quasipotential approach[2,3] we shall assume[4] that the relative momentum of hadron interaction is three-dimensional and belongs to the Lobachevsky space. So, there is a relativistic analog of the Rutherford formula

$$T(s,t) = -\frac{m(s)}{4\pi} \int d\mu\,(\vec{r})\, T(s,\vec{r})\, \overset{+}{\xi}(\vec{t},\vec{r}) \,, \qquad (1)$$

where $\xi(\vec{t},\vec{r})$ is the relativistic plane wave, $m(s)$ is the effective mass of the problem, s and t are usual Mandelstam's variables.

Roughly speaking, in the dynamical relativistic Fourier analysis there appears the relative rapidity [3,4]

$$\chi = \ln \frac{\sqrt{m^2 + q^2} + q}{m}$$

instead of the relative momentum in nonrelativistic Fourier analysis. So the relativistic analog of the Heisenberg relation for momentum and coordinate is the uncertainty relation for the rapidity and relativistic relative coordinate

$$\Delta\chi \, \Delta r \geq \frac{1}{2} \frac{h}{mc} .$$

The exponential-power behaviour of the elastic scattering amplitude with increasing momentum transfer has a simple geometrical origin due to the well-known statement: the Euclidean geometry is the local geometry of the Lobachevsky space.

Because of the clear quantum-mechanical meaning of formula (1) we can start to model the elastic scattering amplitude in the relative coordinate space. Comparing with the experimental data in momentum space by the numerical analysis it is possible to construct the elastic amplitude.

If we propose that $T(s,\vec{r})$ has the form

$$T(s,r) = \frac{\Lambda_1(s) e^{-\mu_1(s) r}}{R_1^2(s) + r^2} + \frac{\Lambda_2(s) e^{-\mu_2(s) r}}{R_2^2 s) - r^2}, \qquad (2)$$

then $T(s,t)$ factorizes in the form [5]

$$T(s,t) = T(s,t,A,R(s)), \qquad (3)$$

where A is a set of unknown parameters and

$$R(s) = R_1 + R_2 / s^{R_3} + R_4 (\ln s / R_5)^{R_6} . \qquad (4)$$

The optical theorem gives [6] from (3)

$$\sigma_t(s) = 2\pi R^2(s). \qquad (5)$$

So, the function $R(s)$ can be interpreted as an effective radius of hadronic interactions.

The effective radius of hadron-hadron interactions above the threshold energies has been obtained [7] in the form

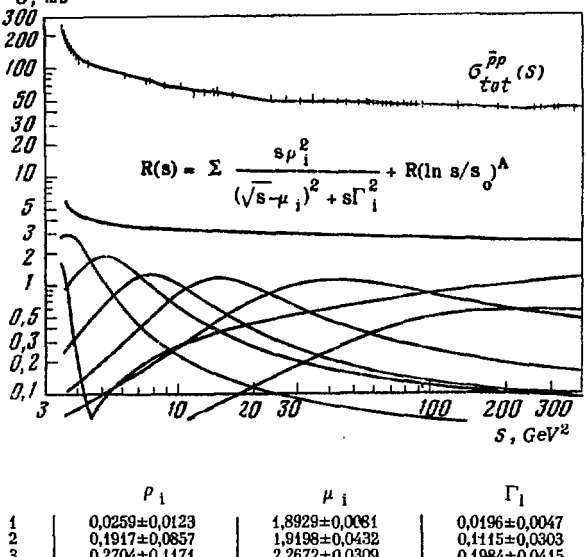

	ρ_i	μ_i	Γ_i
1	0,0259±0,0123	1,8929±0,0061	0,0196±0,0047
2	0,1917±0,0857	1,9198±0,0432	0,1115±0,0303
3	0,2704±0,1171	2,2672±0,0309	0,1984±0,0415
4	0,2703±0,1150	2,7916±0,0296	0,2431±0,0483
5	0,3464±0,1041	3,8160±0,0764	0,3282±0,0536
6	0,6315±0,1114	6,4937±0,1362 *	0,6157±0,0643 *
7	0,8842±0,0882	15,0292±0,3446 *	1,1628±0,0312 *

$R = 0{,}2428 \pm 0{,}0023$ mb$^{1/2}$ *, $A = 0{,}9993 \pm 0{,}0030$ *
$R_0 = 0{,}906 \pm 0{,}353$ mb$^{1/2}$

Fig. 1

$$R(s) = \sum_{i=1}^{n} \frac{s\rho_i^2}{(\sqrt{s}-\mu_i)^2 + s\Gamma_i^2} + R \ln^A(s/so). \qquad (6)$$

The unknown functions and parameters have been found by solving the overdetermined nonlinear system of equations

$$\sigma_t^{expt}(s_i) = 2\pi R^2(s_i), \qquad (7)$$

where $\sigma_t^{expt}(s)$ are the experimental total cross sections for the processes $\bar{p}p$, pp, $\pi^{\mp}$, $K^{\mp}p$. The autoregularized itera-

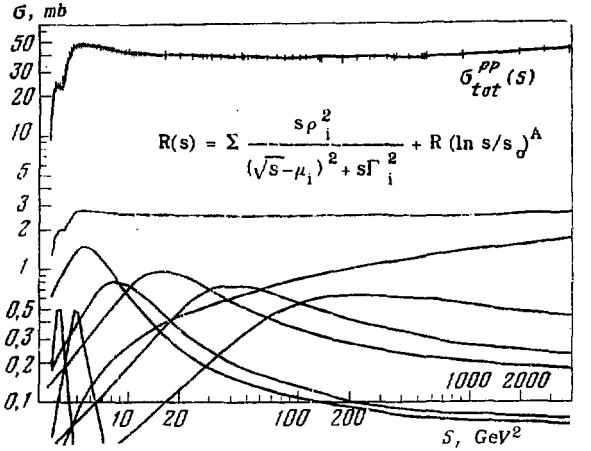

	ρ_i	μ_i ГэВ	Γ_i
1	0,0222±0,0043	1,9691±0,0020	0,0282±0,0040
2	0,0419±0,0100	2,2055±0,0041	0,0586±0,0078
3	0,2580±0,0551	2,3606±0,0361	0,2104±0,0226
4	0,2716±0,2022	2,9249±0,0619	0,3051±0,1056
5	0,4427±0,2098	3,9992±0,1514	0,4555±0,0980
6	0,5234±0,1296	6,4937±0,1362 *	0,6157±0,0643 *
7	0,9221±0,0637	15,0292±0,3446 *	1,1628±0,0312 *

$R = 0{,}2428 \pm 0{,}0023$ $mb^{1/2}$ *, $A = 0{,}9993 \pm 0{,}0030$ *
$R_0 = 0{,}856 \pm 0{,}392$ $mb^{1/2}$

Fig. 2

tion processes of the Gauss-Newton type [8] in the numerical analysis were used.

Figures 1-6 represent the experimental data and our description of the above-mentioned total cross sections, the corresponding effective radii, and their constituents (see (6)). The quantity χ^2/N equals 1.11 for nucleons; 1.01, for pions; 1.06, for kaons. The formula (6) shows that the effective radius is a sum of the "effective radii" of successively opening with the increasing energy "channels"

and the Froissart term. Starting from $s \geq 100$ GeV^2 the Froissart term gives the main contribution to the effective radius. The asymptotic behaviour of the effective radius is

$$R_\infty(s) = R_0 + R \ln^A(s/s_0),$$

$$R_0 = \sum_{i=1}^{7} \frac{\rho_i^2}{1+\Gamma_i^2}.$$

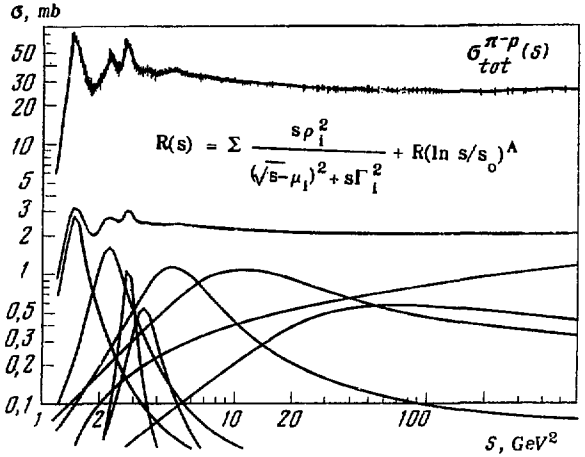

	ρ_i	μ_i	Γ_i
1	0,1073±0,0006	1,2204±0,0003	0,0651±0,003
2	0,1188±0,0012	1,4961±0,0004	0,0952±0,0008
3	0,0351±0,0005	1,6800±0,0003	0,0332±0,0003
4	0,0641±0,0028	1,8430±0,0008	0,0879±0,0022
5	0,2560±0,0166	2,1819±0,0039	0,2423±0,0087
6	0,5992±0,0525	3,3347±0,0212 *	0,5831±0,0326 *
7	0,9055±0,0710	8,3813±0,1397 *	1,2014±0,0406 *

$R = 0{,}1814 \pm 0{,}0024$ mb$^{1/2}$ *, $A = 0{,}9996 \pm 0{,}0043$ *
$R_0 = 0{,}696 \pm 0{,}087$ mb$^{1/2}$

Fig. 3

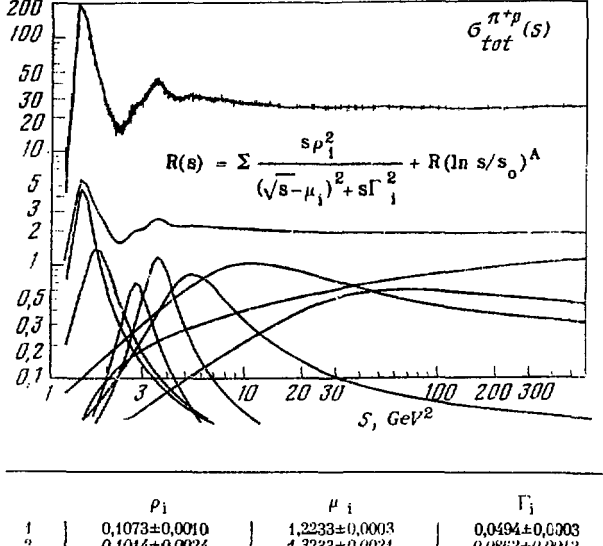

	ρ_i	μ_i	Γ_i
1	0,1073±0,0010	1,2233±0,0003	0,0494±0,0003
2	0,1014±0,0024	1,3233±0,0021	0,0862±0,0013
3	0,0676±0,0017	1,6700±0,0007	0,0831±0,0014
4	0,0906±0,0008	1,8993±0,0004	0,0849±0,0005
5	0,1958±0,0129	2,3490±0,0020	0,2185±0,0064
6	0,5863±0,0508	3,3347±0,0212 *	0,5831±0,0326 *
7	0,9176±0,0709	8,3813±0,1397 *	1,2014±0,0406 *

$R = 0{,}1814 \pm 0{,}0024$ mb$^{1/2}$ *, $A = 0{,}9996 \pm 0{,}0043$ *
$R_0 = 0{,}672 \pm 0{,}082$ mb$^{1/2}$

Fig. 4

Obviously, comparing the behaviour of the total cross sections and the asymptotical ones the value of the Froissart energy can be estimated. The asymptotic behaviour for all total cross sections is reached (see Fig. 7) in the energy range $s = 10^5 \div 10^6$ GeV^2 ($\sqrt{s} = 300$-1000 GeV, $10^{-16} \div 10^{-17}$ cm). If one compares the Froissart energy with the unitary limit energy for the weak interactions, then it is possible to interpret the Froissart energy as the threshold energy of new structures of matter.

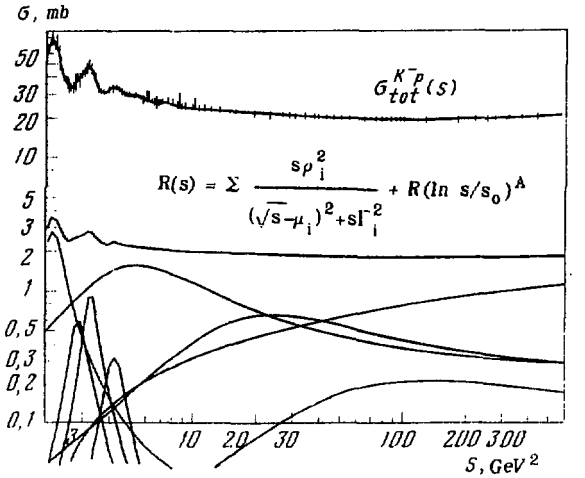

	ρ_i	μ_i	Γ_i
1	0,1038±0,0031	1,4836±0,0015	0,0619±0,0015
2	0,0411±0,0024	1,6985±0,0010	0,0528±0,0022
3	0,0419±0,0014	1,8146±0,0006	0,0431±0,0010
4	0,0324±0,0011	2,0640±0,0006	0,0573±0,0011
5	0,5421±0,0281	2,3310±0,0092	0,4331±0,0158
6	0,5663±0,1093	4,9226±0,1100 *	0,7006±0,0943 *
7	0,5412±0,1468	11,4578±0,3851 *	1,1793±0,1192 *

$R=0,1941\pm0,0052$ $mb^{1/2}$ *, $A=0,9998\pm0,0036$ *
$R_0=0,600\pm0,140$ $mb^{1/2}$

Fig. 5

Figure 8 shows that the theoretical description confirms the Pomeranchuk theorem. The solid curve represents the lower bound; and the dotted one, the upper bound of the corresponding cross sections.

The dependence of the effective radius on the quantum numbers has been obtained in [9]. The total cross sections of $\bar{p}, p, \pi^{\mp}, K^{\mp}$ with proton, neutron, deutron for $s \geq 100$ GeV^2

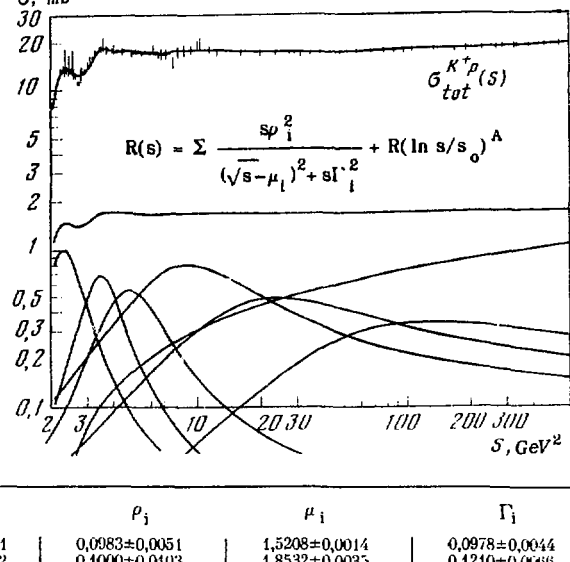

	ρ_i	μ_i	Γ_i
1	0,0983±0,0051	1,5208±0,0014	0,0978±0,0044
2	0,1000±0,0103	1,8532±0,0035	0,1210±0,0066
3	0,1435±0,0298	2,1694±0,0126	0,1930±0,0207
4	0,0	2,3738±1,8847	0,2305±0,8315
5	0,3865±0,0659	2,9879±0,0428	0,4322±0,0497
6	0,4933±0,1109	4,9226±0,1100 *	0,7006±0,0943 *
7	0,7000±0,1418	11,4578±0,3851 *	1.1793±0,1192 *

$R=0{,}1941\pm0{,}0052$ mb $^{1/2}$ *, $A=0{,}9998\pm0{,}0036$ *
$R_0=0{,}533\pm0{,}167$ mb $^{1/2}$

Fig. 6

can be described as functions of the quantum numbers with the formula (5) and

$$R(s,A,\alpha) = R_1 + R_2/(s/R_5)^{R_3} + R_4 \ln(s/R_5), \qquad (8)$$

where α is a set of quantum numbers and A, a set of parameters. The functions $R_i (i = 1,\ldots,5)$ have the form

$$R_1 = A_1 M + A_2 J + A_3 I + A_4 S$$

$$R_2 = A_5 + A_6 K + A_7 |B| + A_8 |Q| + A_9 |I3| + A_{10} |Y|$$

$$R_3 = A_{11} + A_{12}M + A_{13}J + A_{14}|Q| + A_{15}I + A_{16}|I3| + A_{17}|S|$$

$$R_4 = A_{18} + A_{19}K + A_{20}I$$

$$R_5 = I + A_{21},$$

where

$M = m_1 + m_2$	mass
$B = b_1 + b_2$	baryon number
$J = (J_1 + J_2)(J_1 + J_2 + 1)$	spin
$Q = q_1 + q_2$	charge
$I = (I_1 + I_2)(I_1 + I_2 + 1)$	isotopic spin
$I3 = I3_1 + I3_2$	third projection of isotopic spin
$K = k_1 + k_2$	SU(3) quark number
$Y = y_1 + y_2$	hypercharge
$S = s_1 + s_2$	*strangeness*

AP.P,PI$^-$,PI$^+$,K$^-$,K$^+$ –PROTON FROIASSART ENERGIES

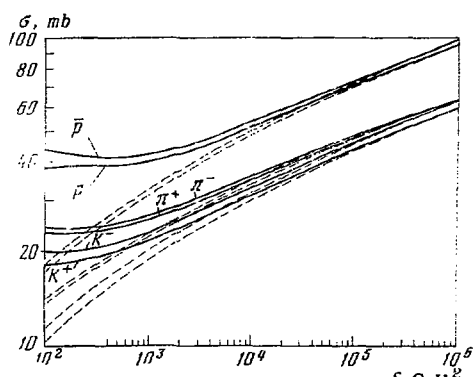

Fig. 7

The Table represents the values and the errors of the parameters A. The quantity χ^2/N is 1.11. Figures 9-11 represent the obtained description of the experimental data.

Table

N	A_i	+/-	ΔA_i	N	A_i	+/-	ΔA_i
1	.7111	+/-	.0146	11	.3218	+/-	.0105
2	-.2319	+/-	.0122	12	.0479	+/-	.0070
3	.0226	+/-	.0023	13	-.0708	+/-	.0034
4	-.3744	+/-	.0110	14	-.0184	+/-	.0003
5	2.4850	+/-	.0388	15	.0329	+/-	.0017
6	.1873	+/-	.0037	16	.0250	+/-	.0011
7	.0171	+/-	.0023	17	.0705	+/-	.0028
8	-.3796	+/-	.0092	18	.1762	+/-	.0015
9	.4035	+/-	.0217	19	.0055	+/-	.0001
10	-.2193	+/-	.0034	20	-.0049	+/-	.0005
				21	.8100	+/-	.0570

(For the dimensions of the parameters see formula (8))

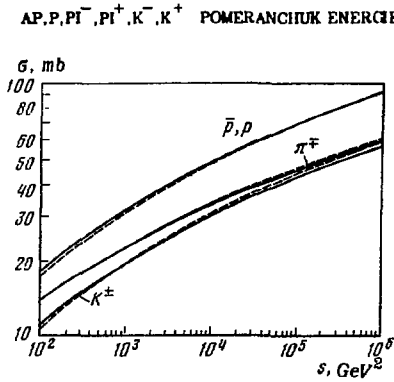

Fig. 8

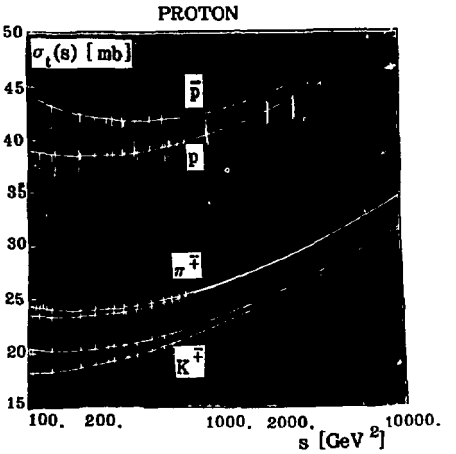
PROTON
$\sigma_t(s)$ [mb]
$\bar{p}$
p
$\pi^{\mp}$
$K^{\mp}$
50
45
40
35
30
25
20
15
100.
200.
1000.
2000.
10000.
s [GeV^2]

Fig. 9

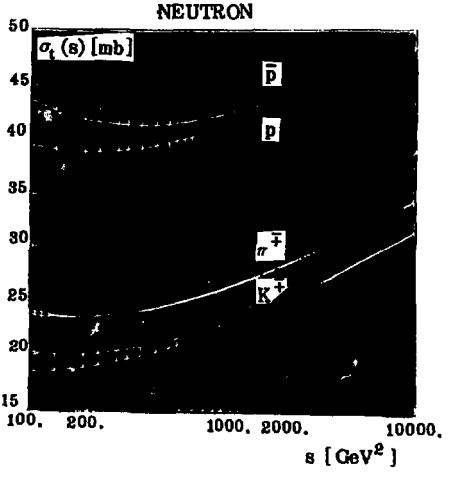
NEUTRON
σ_t (s) [mb]
$\bar{p}$
p
$\pi^{\mp}$
$K^{\mp}$
50
45
40
35
30
25
20
15
100.
200.
1000.
2000.
10000.
s [GeV^2]

Fig. 10

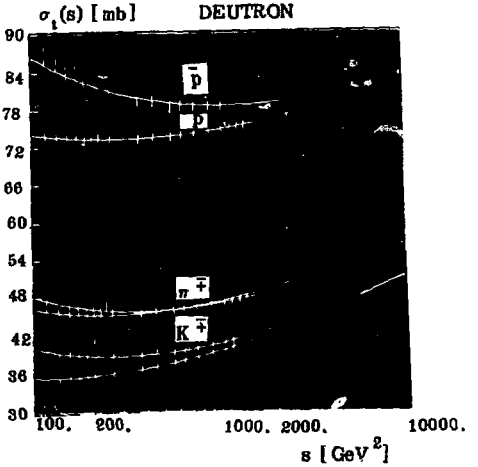
σ_t(s) [mb]
DEUTRON
90
84
78
72
66
60
54
48
42
36
30
$\bar{p}$
p
$\pi^{\mp}$
$K^{\mp}$
100.
200.
1000.
2000.
10000.
s [GeV^2]

Fig. 11

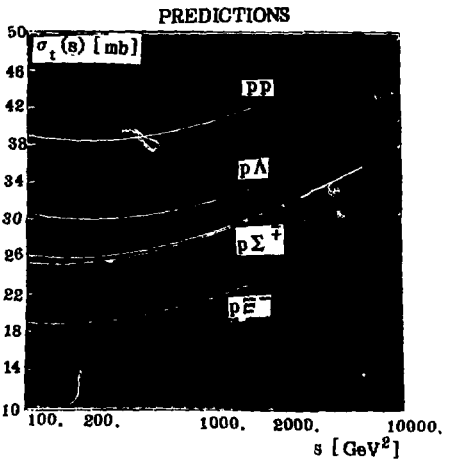
PREDICTIONS
σ_t(s) [mb]
50
46
42
38
34
30
26
22
18
14
10
pp
pΛ
pΣ^+
pΞ^-
100.
200.
1000.
2000.
10000.
s [GeV^2]

Fig. 12

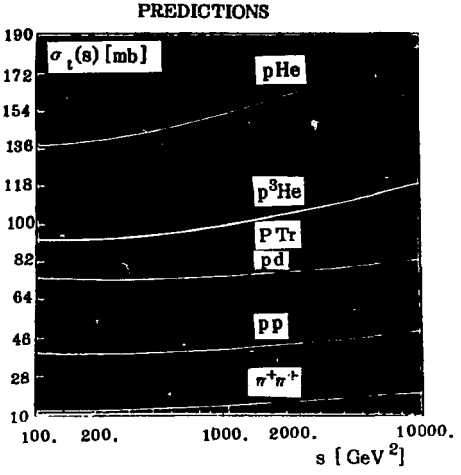
PREDICTIONS
$\sigma_t(s)$ [mb]
pHe
p^3He
PTr
pd
pp
$\pi^+\pi^-$
190
172
154
136
118
100
82
64
46
28
10
100.
200.
1000.
2000.
10000.
s [GeV^2]

Fig. 13

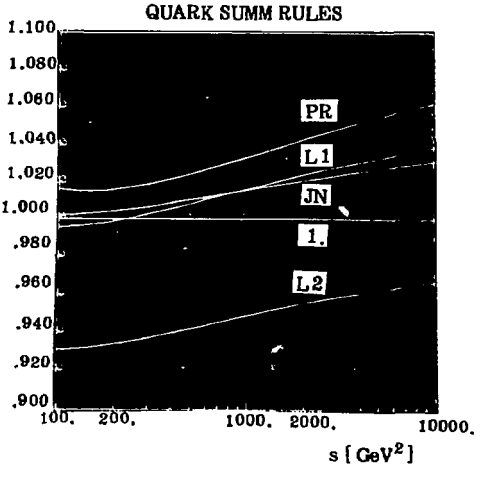
QUARK SUMM RULES
PR
L1
JN
1.
L2
1.100
1.080
1.060
1.040
1.020
1.000
.980
.960
.940
.920
.900
100.
200.
1000.
2000.
10000.
s [GeV^2]

Fig. 14

Figure 12 represents the predictions for the total cross sections of Λ, Σ^+, Ξ^- hyperons with proton. Figure 13 represents our predictions for the total cross sections of Tr, ^3He, He with proton and of $\pi^+\pi^+$ interaction. Figure 14 represents the behaviour of the following quark sum rules[10]

$$PR: \quad 6\,\pi N = 3\,KN + 2\,NN$$

$$L1: \quad 6\pi^- p + 3K^+ p = 2pn + 6\,K^- p$$

$$L2: \quad pp + \Sigma^- p = \Lambda p + pn$$

$$JN: \quad 4\pi^+ p = 2\pi^- p + 7/8\,K^+ p + 3/4\,pp.$$

In conclusion it should be mentioned that our predictions have about 10% uncertainty. The future measurements of the hadron-hadron total cross sections at $s = 400$ to 1000 GeV^2 would decrease this uncertainty.

REFERENCES

1. Боголюбов Н.Н. Теория симметрии элементарных частиц. В сб.: Физика высоких энергий и теория элементарных частиц. "Наукова думка", Киев, 1967.
2. Logunov A.A., Tavkhelidze A.N. Nuovo Cim.,1963,29, p.380. Кадышевский В.Г., Тавхелидзе А.Н. В сб.: Проблемы теоретической физики. "Наука", М., 1969.
3. Kadyshevsky V.G. Nucl.Phys., 1968, B86, p.125; Kadyshevsky V.G., Mateev M.D. Nuovo Cim., 1967, 55A,p.276; Кадышевский В.Г., Мир-Касимов Р.М., Скачков Н.Б. ЭЧАЯ, 1972, том 2, вып.3, с.637.
4. Mavrodiev S.Cht. Fizika, 1977, p.11.
5. Mavrodiev S.Cht. JINR, P2-8897, Dubna, 1975.
6. Alexandrov L., Mavrodiev S.Cht. JINR, E2-9936, Dubna,1976.
7. Drenska S., Mavrodiev S.Cht. Yad. fiz., 1978, v.28,p.749.
8. Александров Л. ЖВМ и МФ, 1971, 11, с.1; Александров Л. ОИЯИ, Р5-5511, Дубна, 1970; Александров Л. ОИЯИ, Б1-5-9969, Дубна, 1976.
9. Alexandrov L., Drenska S., Mavrodiev S.Cht. JINR, P2-12721, Dubna, 1979.
10. Denisove S.P. et al. Nucl.Phys., 1973, B65, p.1; Lipkin H.J. Nucl.Phys., 1974, B79, p.381. Kang R., Nikolescu J. Phys.Rev., 1975, D11, p.2461.

Received by Publishing Department
on October 5 1979.